NATIONAL TRANSPORTATION SAFETY BOARD
Office of Research and Engineering
Materials Laboratory Division
Washington, D.C. 20594

March 26, 2020

MATERIALS LABORATORY FACTUAL REPORT Report No. 19-025

A. ACCIDENT INFORMATION

Place	:	Firebaugh, California
Date	:	May 15, 2017
Vehicle	:	Lancair Evolution
NTSB No.	:	WPR17LA104
Investigator	:	Stephen Stein, AS-WPR

B. COMPONENTS EXAMINED

Windshield pieces and windshield frame.

C. DETAILS OF THE EXAMINATION

An overall view of the submitted windshield pieces and windshield frame is shown in figure 1. The windshield fractured in flight, and most of the windshield was missing from the submitted pieces. The windshield frame had been cut from the airplane fuselage, and before the components were submitted for examination at the NTSB Materials Laboratory, they had been sent to the National Institute for Aviation Research at Wichita State University in Wichita, Kansas, for examination and analysis. Several areas of the frame and windshield had been sectioned for that examination and analysis.

The windshield was manufactured from cast acrylic, and the windshield frame was manufactured primarily with a carbon fiber reinforced polymer (CFRP) with layers of carbon-fiber fabric and epoxy. The outer two inches around the edges of the windshield were bonded in place with a blue adhesive at the exterior surface of the windshield and a clear adhesive at the interior surface. According to window installation instructions, the exterior surface of the windshield is bonded in place with Hysol EA 9360 paste epoxy,[1] and the interior surface of the windshield is bonded in place with Rhino 1307-LV resin plus hardener.[2]

Pieces of the windshield were examined visually, and directions of fracture propagation were determined using fracture features including hackles, rib lines, and Wallner lines.[3] Unlabeled arrows in figure 1 indicate directions of fracture propagation on

[1] Henkel Corporation, Bay Point, California.
[2] Rhino Linings Corporation, San Diego, California.
[3] Hackles are radial features that form as a crack front diverges into different planes as a form of energy dissipation during slow or rapid fracture. Rib lines are curving features representing a crack front during slow

the pieces shown. The small separate pieces shown in the middle of the frame in figure 1 were from the upper aft side of the frame to the right of the centerline.

A closer view of the windshield piece at the left side of the frame is shown in the lower right image in figure 1. The windshield piece included a longitudinal fracture that extended upward and aft, and the fracture was labeled fracture A for reference. The forward end of fracture A was visible within the windshield slot in the frame adjacent to one of the sample cutouts. A view of the forward end of fracture A within the windshield slot is shown in figure 2.

A crack in the left windshield piece was observed adjacent to the frame on the lower left side of the windshield and was labeled fracture B for reference as indicated in the lower right image in figure 1 and in a closer view in figure 3. To facilitate an examination of fracture B, the windshield frame was cut forward and aft of the windshield piece, and a chisel was used to pry open the windshield slot to facilitate separation of the windshield piece from the slot. The windshield piece was then pulled out of the slot as shown in figure 4.

In figure 4, the fractures on the left windshield piece are shown labeled with letters for reference (including fractures A and B labeled in figure 1), and unlabeled arrows indicate fracture propagation directions. Fracture B had an origin located near the aft end of the crack as indicated in figure 4, a location that had been within the frame slot. From the origin area, fracture B propagated forward to fracture C and aft to fracture E. Based on the geometry of fracture intersections and fracture features at the intersections, fractures C, D, and E were secondary to fractures A and B.

A photograph of the aft end of fracture B including the origin area is shown in figure 5. Ratchet marks emanated from the interior surface at the origin area, indicating fracture initiation on multiple slightly offset planes from the interior surface. The fracture progressed toward the exterior surface as the fracture front extended forward and aft as indicated by unlabeled arrows in figure 5. The overall progression from interior to exterior along the length of crack B was consistent with higher tension stress at the interior surface relative to the exterior, indicative of a combination of tension and bending loads during fracture.

An optical image of the fracture B origin area is shown at higher magnification in figure 6. Hackles and Wallner lines were observed on the fracture surfaces emanating from the origin area, features consistent with rapid overstress fracture.

The left windshield piece was cut using a bandsaw to section the aft end of the fracture B fracture surface, including the origin area, from the rest of the piece to facilitate an examination using a scanning electron microscope (SEM). SEM images of the origin area are shown in figures 7 through 10. Fracture features at the aft end of the origin area were rubbed consistent with post-fracture recontact as shown in figure 8. However, the

or rapid fracture. Wallner lines are faint curving ridges on the surface that form during rapid crack growth due to crack front interactions with reflected energy waves.

fracture surface showed evidence of microductility with small tear ridges, dimple features, and parabolic marks.[4] At the forward end of the origin area, the fracture surface showed similar evidence of microductility with limited rubbing damage. Figure 10 shows fracture features close to the interior surface where a parabolic mark was observed.

The lower left edge of the windshield piece with the mating side of fracture B remained held within the windshield frame piece shown in figure 4. In order to remove the piece from the frame, the two sides of the frame slot were pulled apart by hand to separate the interior CFRP layers from the skin layers on the exterior side of the windshield slot. The remaining windshield piece was then removed from the frame, and the forward ends of the pieces are shown in figure 11 with mating sides of fracture B positioned in close proximity. As shown in figure 11, the forward end of fracture B intersected the forward edge of the windshield near the start of fracture A. However, the portion of fracture A forward of fracture C was missing. Therefore, it was inconclusive whether fracture A could have initiated as a result of fracture B.

An overall view of the forward lower end of fracture A is shown in the upper image in figure 12. The fracture was flat and perpendicular to the interior and exterior surfaces across the thickness of the windshield along the length of the fracture consistent with fracture under primarily tension loading. At the forward lower end of the fracture shown in the middle left image in figure 12, Wallner lines and hackles were observed consistent with rapid fracture that transitioned to a mirror-like fracture further aft as shown in the lower left image in figure 12. The fracture features were consistent with fracture progressing primarily parallel to the interior and exterior surfaces, also consistent with fracture under primarily tension loading.

Fracture C intersected the forward end of fracture A at a sharp angle and appeared to intersect existing Wallner lines consistent with fracture C occurring secondary to fracture A. A montage of SEM images of the forward end of fracture A is shown at the right in figure 12. The local directions of fracture progression adjacent to fracture C were parallel across the thickness consistent with an origin to fracture A located forward of fracture C. However, an area of the interior surface adjacent to fractures A and C was fractured with a missing chunk of material. Fracture C originated from the fractured chip. On fracture A, rachet marks emanated from the area of the surface chip consistent with a partial origin from the chipped surface. The area of fracture around the chipped surface appeared visually lighter, and when examined using an optical stereomicroscope, the surface appeared rubbed. While some of the fracture features emanated from the chipped surface, the cracks emanating from the chip appeared to merge with another fracture front that had emanated from an origin area forward of the chip.

According to the windshield installation process, the edges of the windshield within the frame are roughened by hand with 80-grit sandpaper near the edge of the windshield slot. Then a dual-action (DA) sander with 40-grit sandpaper is used to roughen the interior and exterior surfaces that are subsequently bonded to the frame. The instructions further

[4] A parabolic mark is a curved feature with tails pointing in the direction of propagation that forms due to fracture reinitiation ahead of the crack front as the fracture progresses.

indicate the DA sander with 40-grit sandpaper should be used to create a rounded edge to the outer edge of the windshield.

A close view of the windshield edge near where fracture B intersected the forward edge of the windshield is shown in figure 13. The edge of the windshield showed areas with a relatively flat bevel shape with a series of parallel curving grinding marks oriented at a nearly 45-degree angle to the windshield edge. The gouges were inconsistent with a rounded edge from a DA sander with 40-grit sandpaper.

The windshield piece that included the forward edge of the windshield immediately to the right of fracture B was missing. However, an impression of the windshield edge remained intact on the mating Hysol adhesive surface on the window frame. The Hysol adhesive near the forward ends of fractures A and B was examined, and impressions of parallel curving grinding marks inconsistent with a DA sander with 40-grit sandpaper were observed in the area within approximately 2 inches of the forward end of fracture B as shown in figure 14.

During the examination of the windshield, a loose piece of the windshield was removed from the upper right side of the windhshield frame at the area indicated in figure 1, and the removed piece is shown in figure 15. Fractures on the forward side of the piece showed propagation extending toward the aft direction toward the aft edge as indicated by unlabeled arrows in figure 15. Before the NTSB Materials Laboratory examination, the windshield frame had been cut in the area where the windshield piece had been located, and the locations of two cuts that penetrated through part of the thickness are indicated. Additionally, several cracks were noted on the rounded edge of the piece in locations indicated in figure 15, and a closer view of the largest of the cracks is shown in figure 16. At the crack locations, a series of parallel curving grinding marks were observed in a flat bevel to the rounded edge.

After documenting the extent of the largest crack, the cracked piece shown in figure 15 was placed in a vice, and a pair of vice-grips was used to apply a bending force to open the largest crack. The resulting lab-opened crack is shown in figure 17 where a dashed line indicates the boundary between the preexisting crack and the lab fracture. The origin area was located at the flat beveled edge with multiple origins from one of the grinding marks. Aside from hackles and ratchet marks, the fracture surface had a relatively smooth appearance with no evidence of Wallner lines.

An SEM image of the crack origin area is shown in figure 18. Multiple ratchet marks were observed at the origin area consistent with multiple origins initiating on slightly different planes. Further from the origin, twist hackles were observed consistent with mixed-mode loading.[5] Closer views of the origin area are shown in figures 19 and 20, where evidence of microductility including dimple features and parabolic marks were observed between the ratchet marks.

[5] Loading modes in crack growth are mode I (tension), mode II (in-plane shear), and mode III (out-of-plane shear). Mixed mode is a combination of at least 2 modes.

An SEM image from the crack boundary is shown in figure 21. Rib marks were observed on the crack surface such as the marks noted with unlabeled arrows in figure 21. At higher magnification, microductility was observed, but generally fewer parabolic marks were observed as shown in figure 22. In an adjacent area on the lab-fractured portion, many overlapping parabolic marks were observed as shown in figure 23.

To create a reference impact fracture surface, a piece of the windshield was cut with a jeweler's saw to create a v-shaped notch at the edge of a piece. The notched piece was then placed in a vice and struck with a mallet. A view of the resulting fracture is shown in figure 24. The lab impact fracture originated near the point of the "V" as shown in figure 24. Hackles and Wallner lines were observed close to the origin area.

SEM images of the origin area of the lab impact reference fracture surface are shown in figures 25 through 27. Evidence of microductility was observed including dimples and tear ridges at the origin shown in figure 26 and parabolic marks near the origin as shown in figure 27.

A piece of the windshield frame labeled P3 that had been cut from the forward left side of the frame near the forward end of fracture A (see figure 1) was roughly polished to view the layup[6] of the CFRP composite skins on the exterior side of the windshield slot. According to airplane construction drawings, the fuselage skin was a sandwich panel construction with exterior and interior CFRP skins separated by a honeycomb core. However, the location selected for the layup examination was from the area in the panel where the honeycomb was terminated to form a joggle for the windshield. SEM images showing the roughly-polished cross-sections for the exterior skin and the interior skin are shown in figure 28, where the upper image shows the interior skin and lower image shows the exterior skin. The layup observed on the sample cross-section is listed in table 1. The fiber orientations are referenced relative to the longitudinal centerline of the airplane, which was approximately 45 degrees away from the skin surface at the sample location. Therefore, the polished plane shown in figure 28 intersected 0/90 fabric layers at an approximately 45 degree angle and intersected ±45 fabric layers at an orientation nearly parallel to one set of fiber bundles in the weave. The layup for the interior and exterior skins as observed on the polished plane differed from the expected layup schedule, also listed in table 1. The interior skin included 2 more layers than the total number listed in the layup schedule for that location, and the exterior skin included 4 more layers than expected.

Another piece of the windshield frame was cut from a location near the lowermost left point of the frame, and the piece was labeled L1 for reference (see figure 1). The piece was then placed in a lab furnace for 2 hours at 530 C followed by a furnace cool to burn off the resin. The resulting stack of carbon-fiber fabric layers was carefully separated and examined. The layup observed on the L1 sample and the corresponding layup schedule at that location are listed in table 2. The interior skin layers matched the

[6] The reinforcement in the CFRP consists of layers of carbon-fiber fabric held together by an epoxy resin. The layup schedule describes the placement and orientations of the fiber reinforcements in the CFRP.

expected layup for that location, but the exterior skin varied from the expected layup orientations and included 4 additional fabric layers.

Table 1. Layup at P3 location (Listed from Exterior Surface)

Skin Sheet	Observed Layup	Layup Schedule
Exterior	0/90 (1 layer)	±45 (2 layers)
Exterior	±45 (6 layers)	
Exterior	0/90 (1 layer)	0/90 (2 layers)
Exterior	±45 (1 layer)	±45 (1 layer)
Interior	±45 (2 layers)	±45 (1 layer)
Interior	0/90 (3 layers)	0/90 (2 layers)
Interior	±45 (1 layer)	±45 (1 layer)

Table 2. Layup at L1 location (Listed from Exterior Surface)

Skin Sheet	Observed Layup	Layup Schedule
Exterior	0/90 (1 layer)	±45 (2 layers)
Exterior	±45 (2 layers)	
Exterior	0/90 (6 layers)	0/90 (2 layers)
Exterior	±45 (1 layers)	±45 (2 layers)
Interior	±45 (1 layer)	±45 (1 layer)
Interior	0/90 (2 layers)	0/90 (2 layers)
Interior	±45 (1 layer)	±45 (1 layer)

Matthew R. Fox, Ph.D.
Senior Materials Engineer

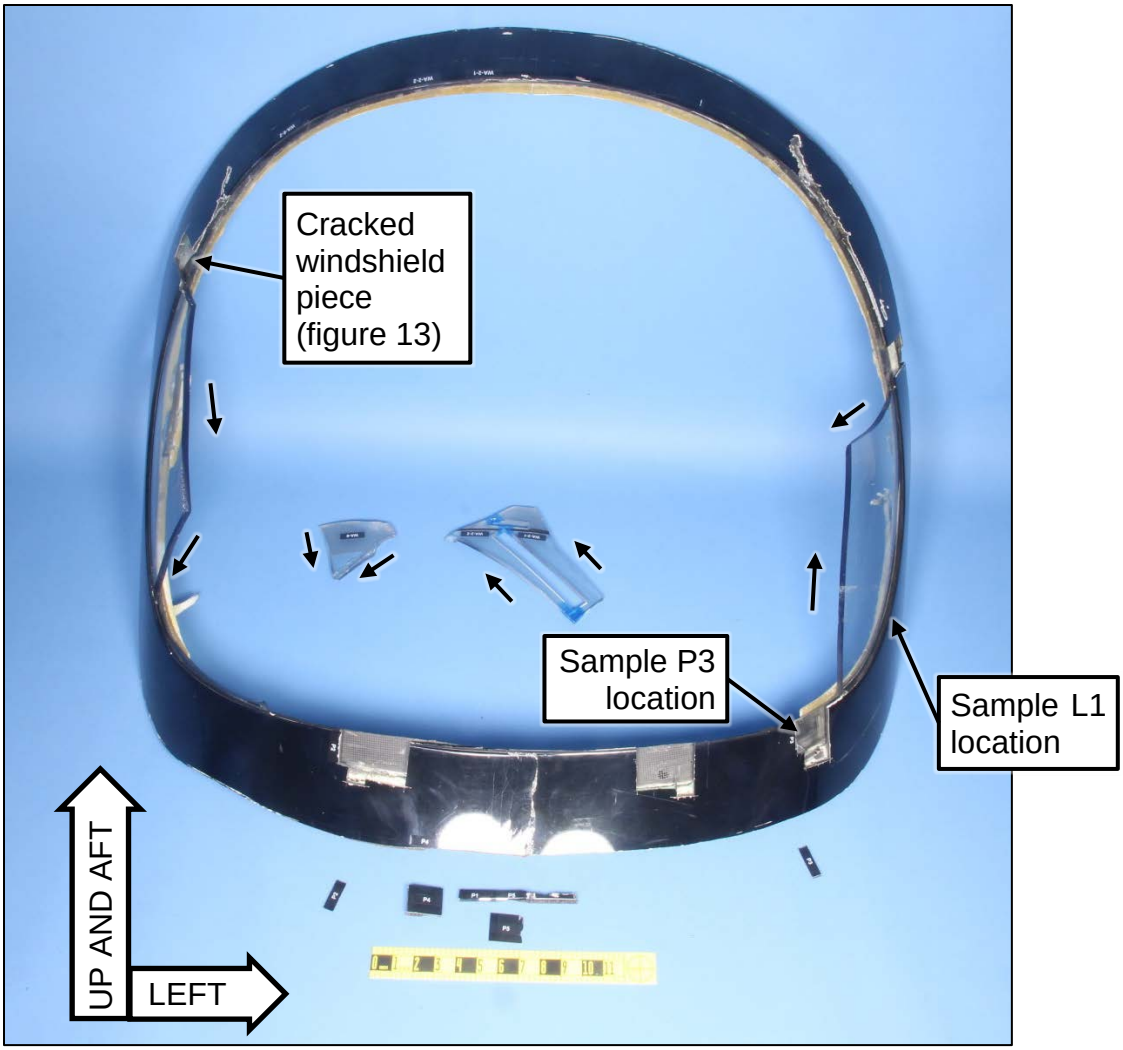

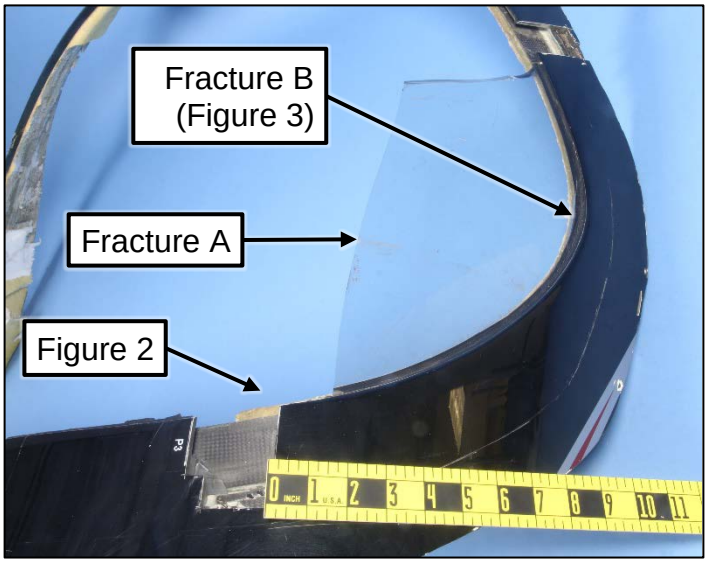

Figure 1. Overall view of the submitted windshield frame and windshield pieces (upper image) with a closer view of the windshield piece at the lower left side of the frame (lower image). Unlabeled arrows in the upper image indicate the directions of fracture propagation.

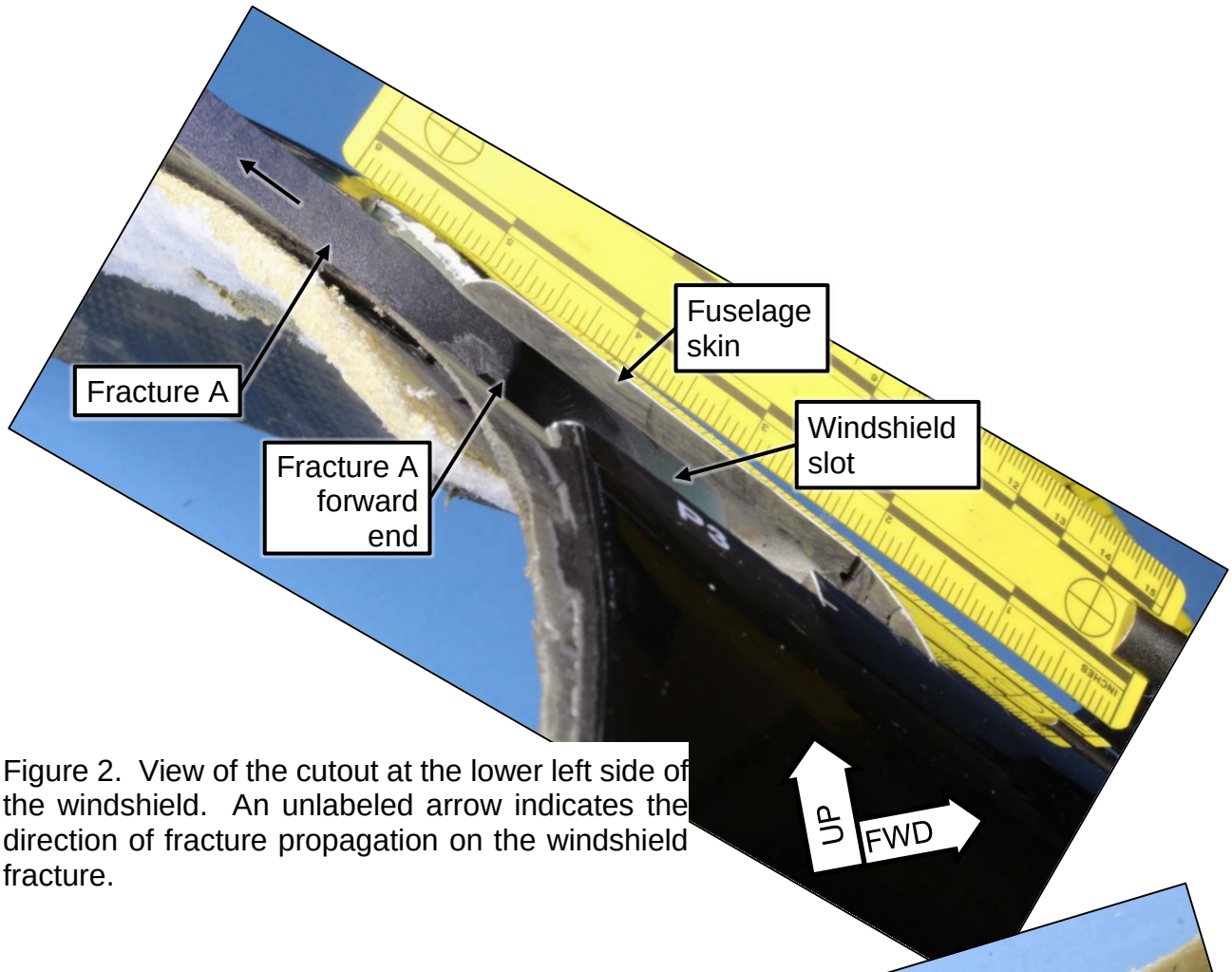

Figure 2. View of the cutout at the lower left side of the windshield. An unlabeled arrow indicates the direction of fracture propagation on the windshield fracture.

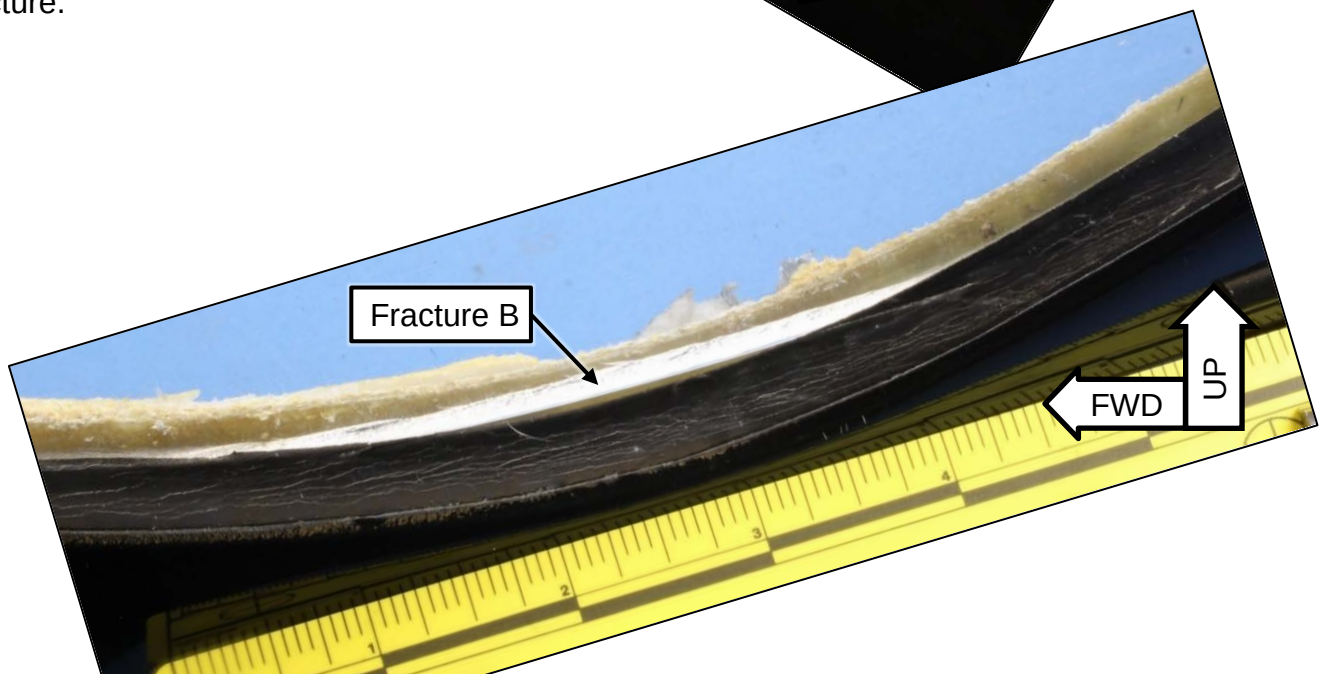

Figure 3. Close view of the left side of the windshield showing fracture B in the windshield next to the window frame.

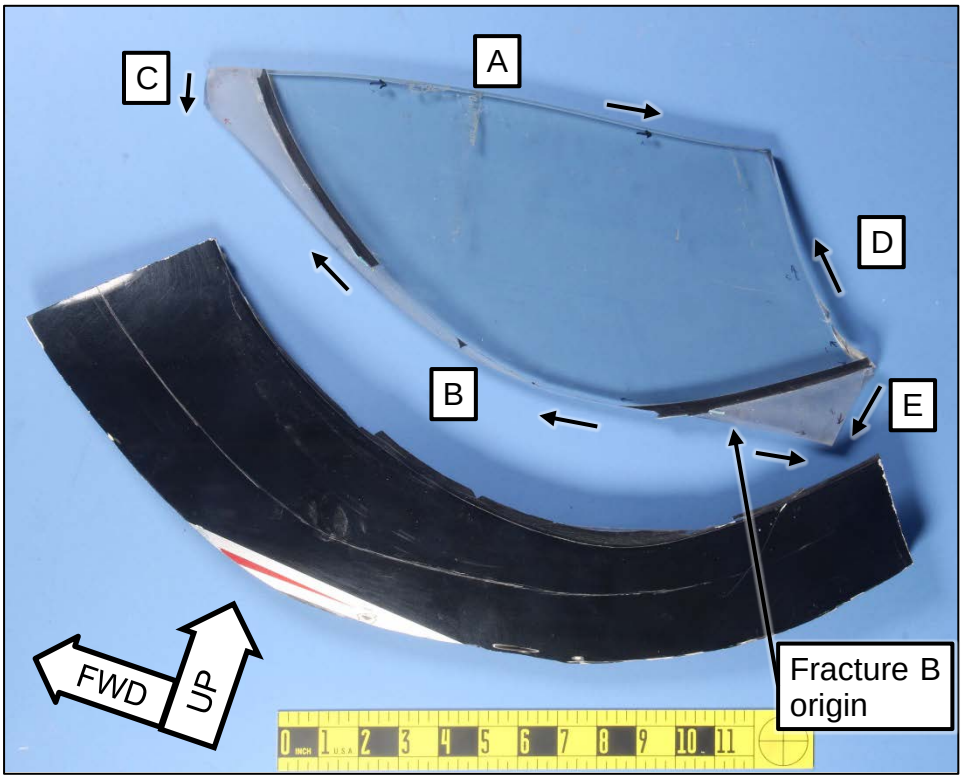

Figure 4. View of the left side of the window frame and windshield piece after the frame was sectioned to facilitate separation of fracture B. Unlabeled arrows indicate directions of fracture propagation. Fracture surfaces on the left windshield piece are labeled A through E for reference in this report.

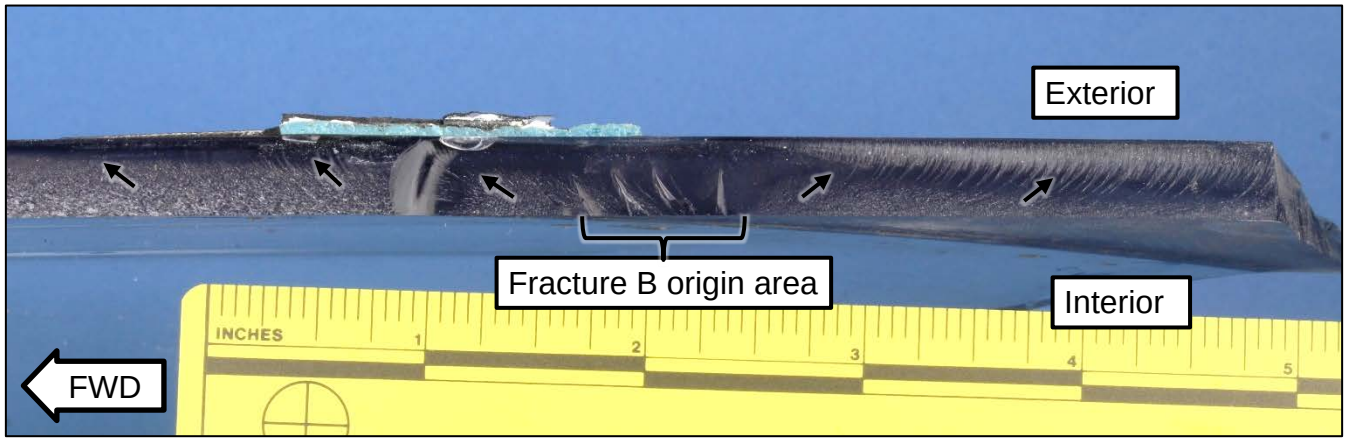

Figure 5. Overall view of the fracture B origin area at the lower left side of the windshield. Unlabeled arrows indicate local fracture propagation directions.

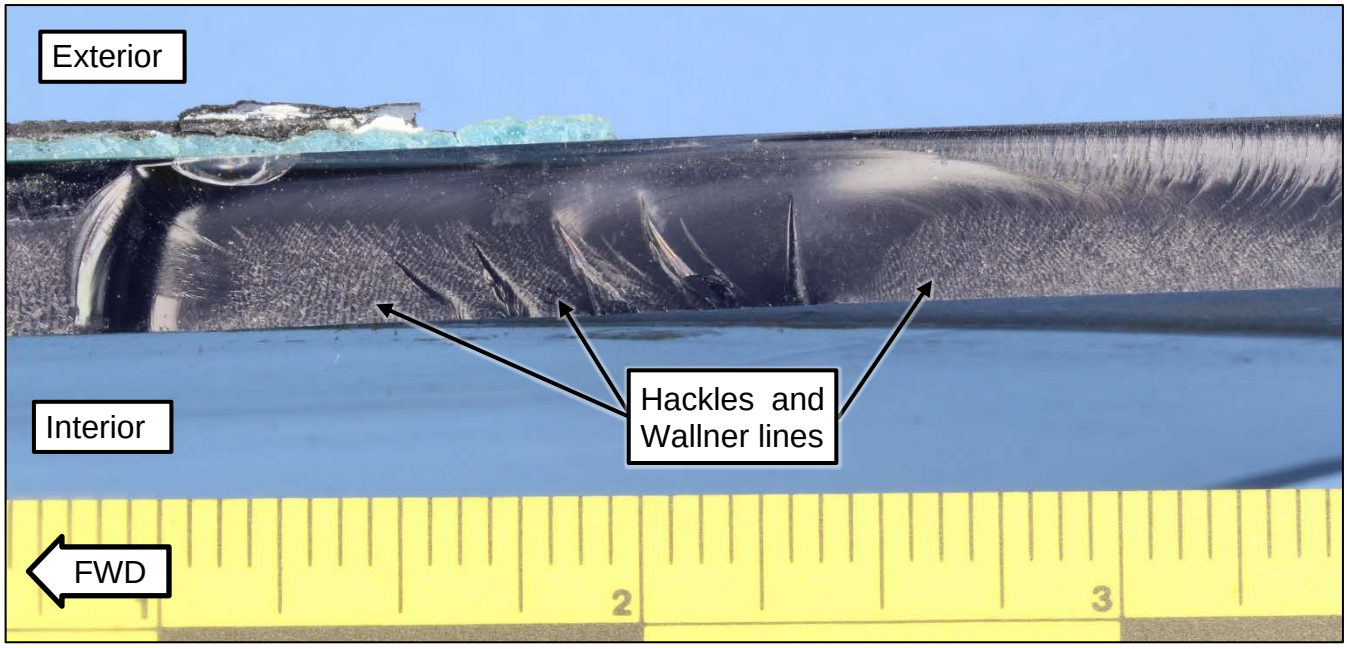

Figure 6. Closer view of the fracture B origin area showing hackles and Wallner lines consistent with rapid fracture.

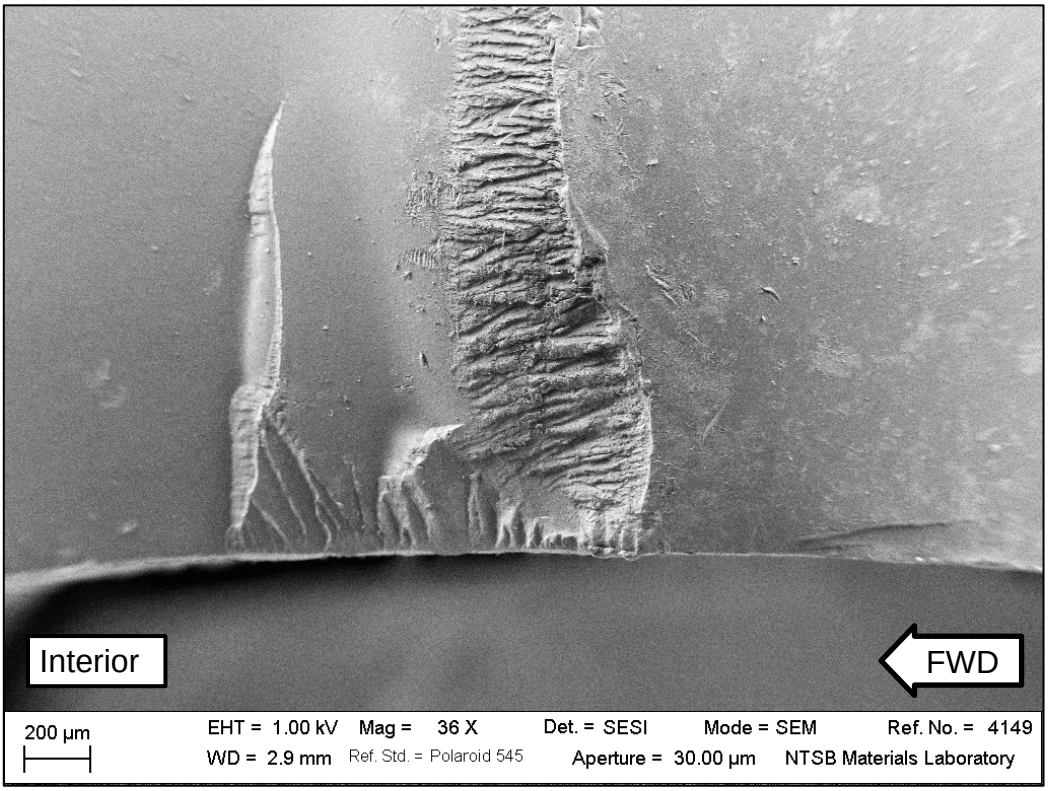

Figure 7. SEM image of the fracture B origin area.

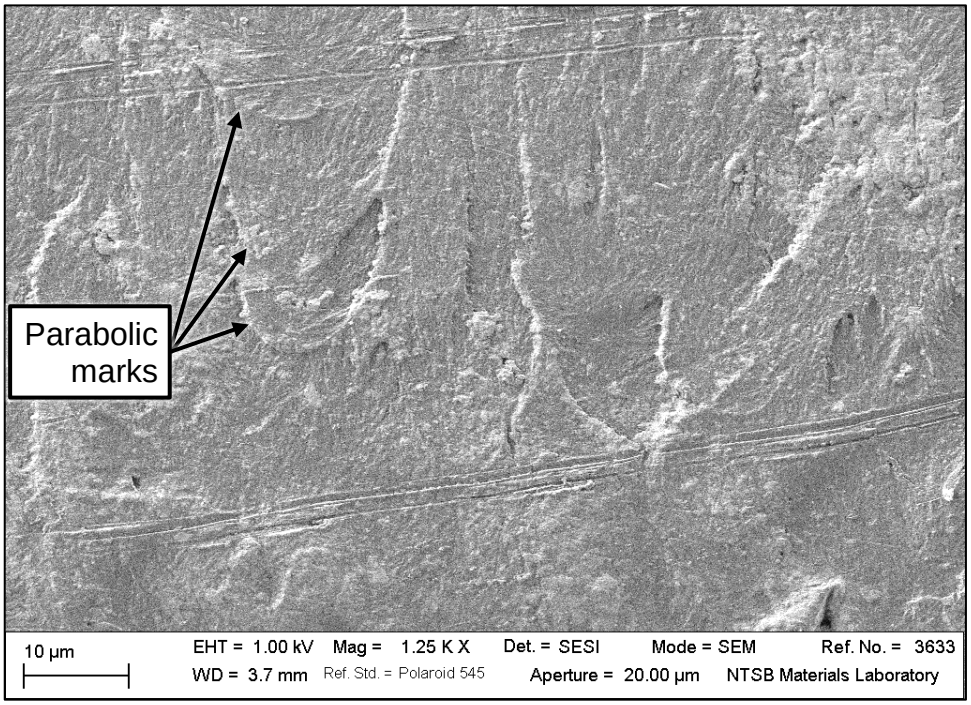

Figure 8. SEM image of fracture features toward the aft end of the fracture B origin area.

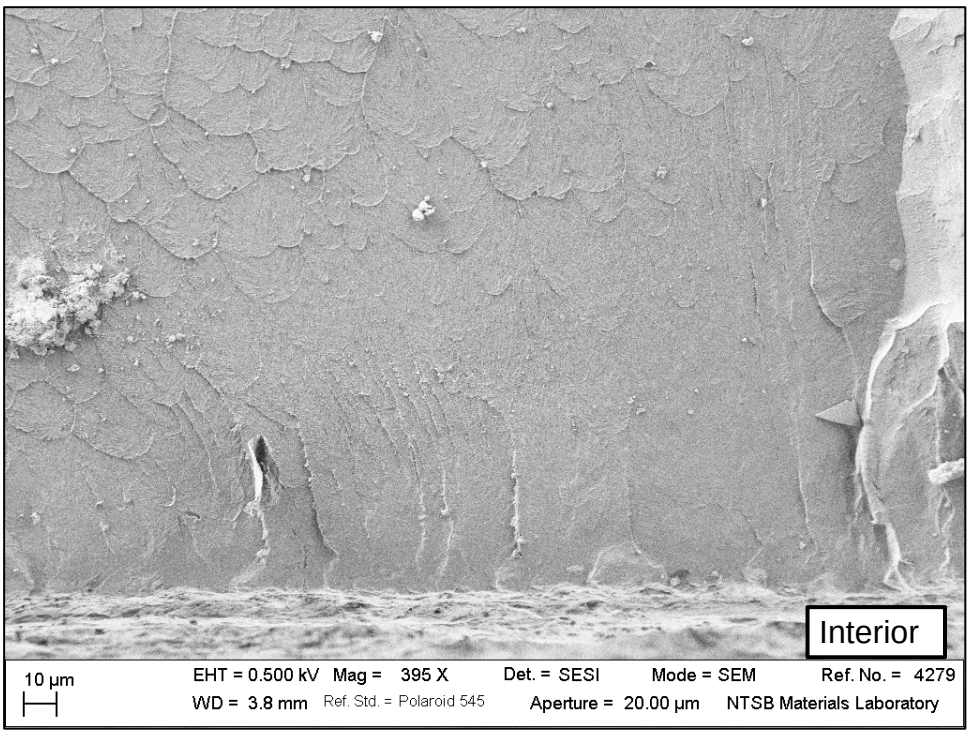

Figure 9. SEM image of fracture features toward the forward end of the fracture B origin area.

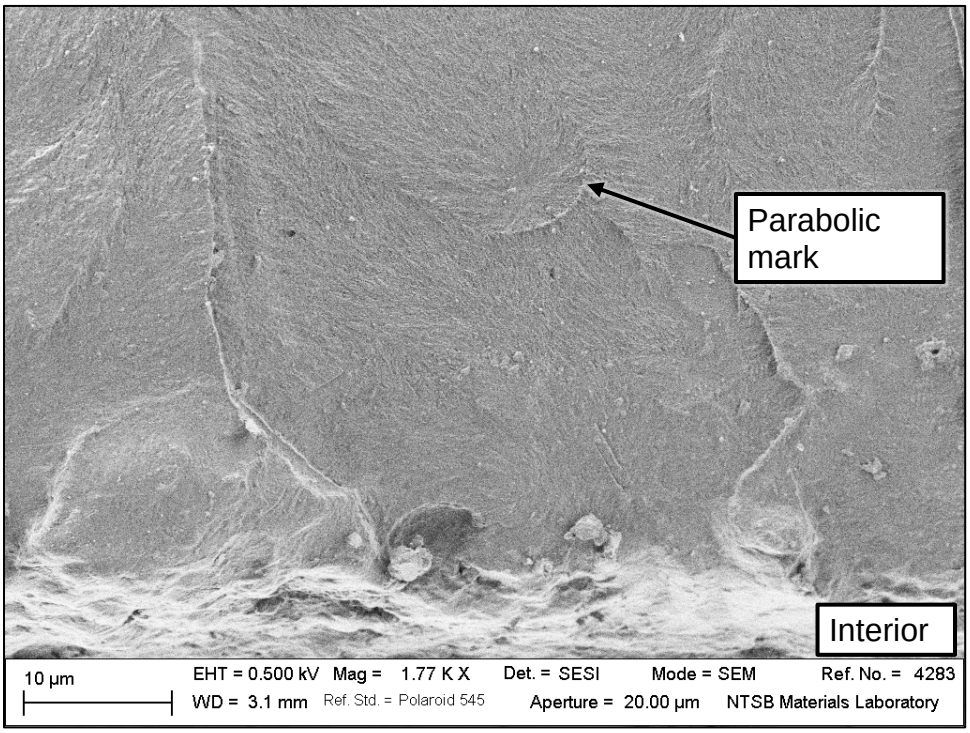

Figure 10. SEM image of fracture features at the forward end of the fracture B origin area shown at higher magnification.

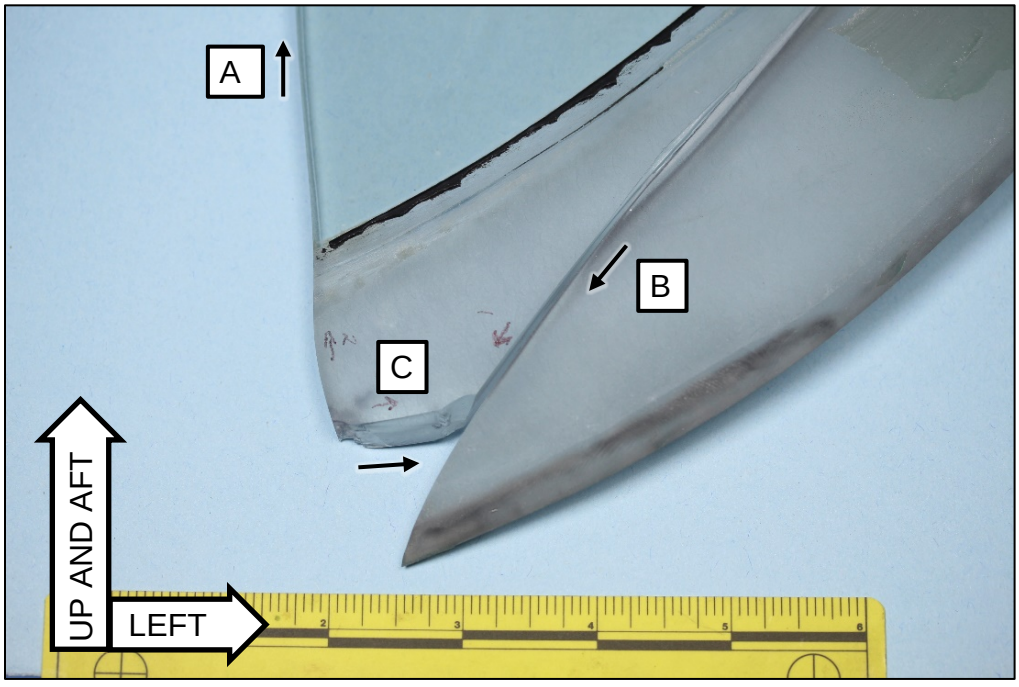

Figure 11. Fracture pattern at the forward end of fracture A and fracture B after both pieces of the windshield with mating sides of fracture B were removed from the windshield frame.

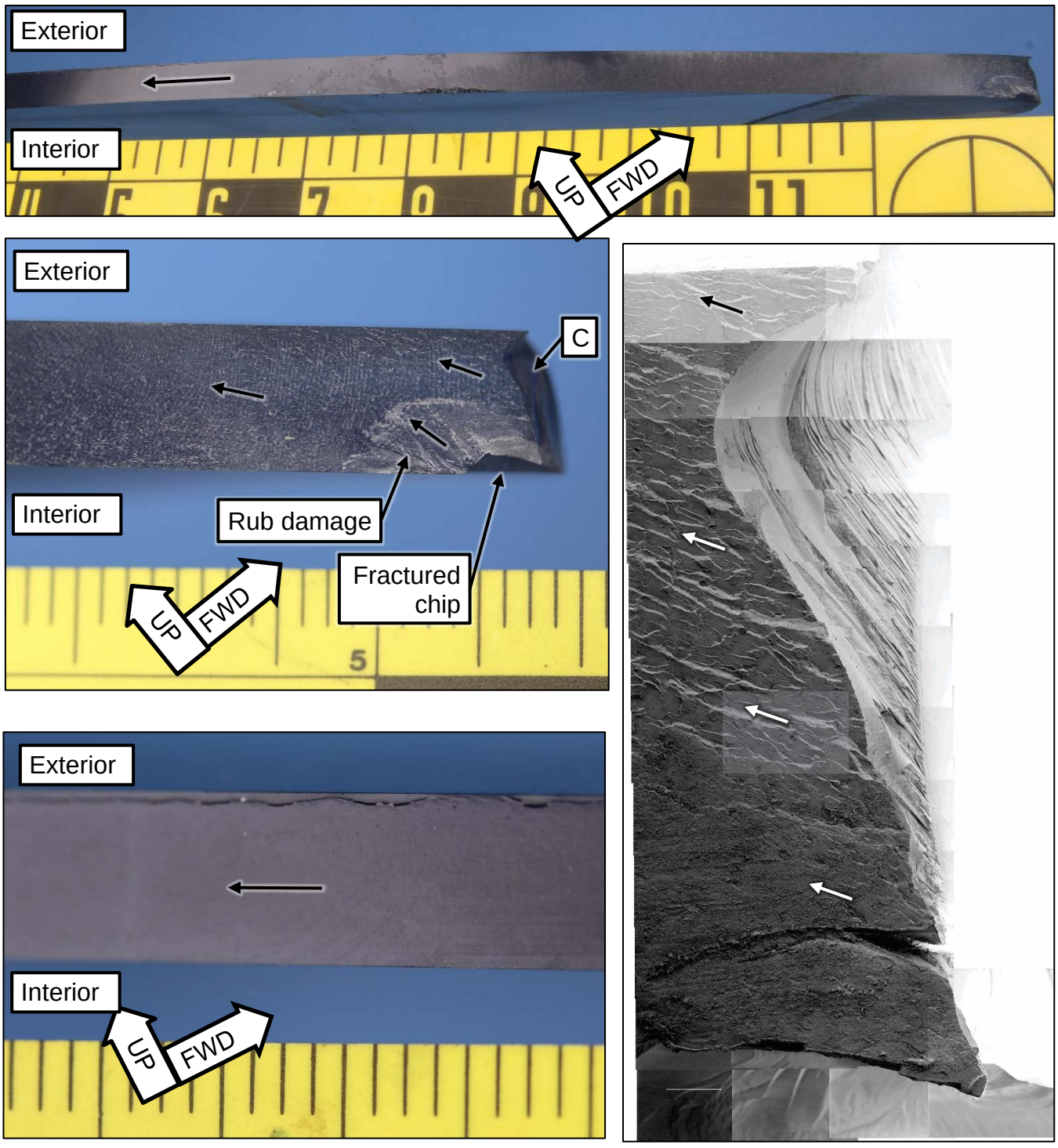

Figure 12. Optical images of the lower forward portion of fracture A showing an overall image (upper image), a view of the beginning of the remaining fracture (middle left image), and fracture features near the middle of the extent of the remaining fracture (lower left image). A mosaic of SEM images of the lower forward end of fracture A is shown at the right. Unlabeled arrows in each image indicate the local direction of fracture propagation.

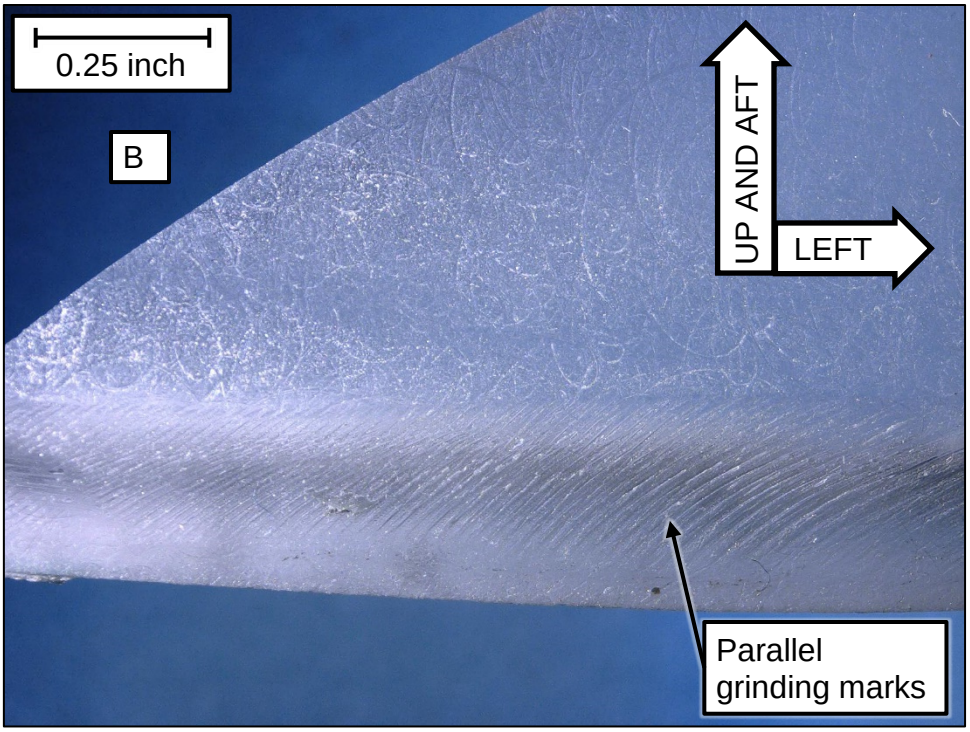

Figure 13. Windshield bevel edge near the forward end of fracture B.

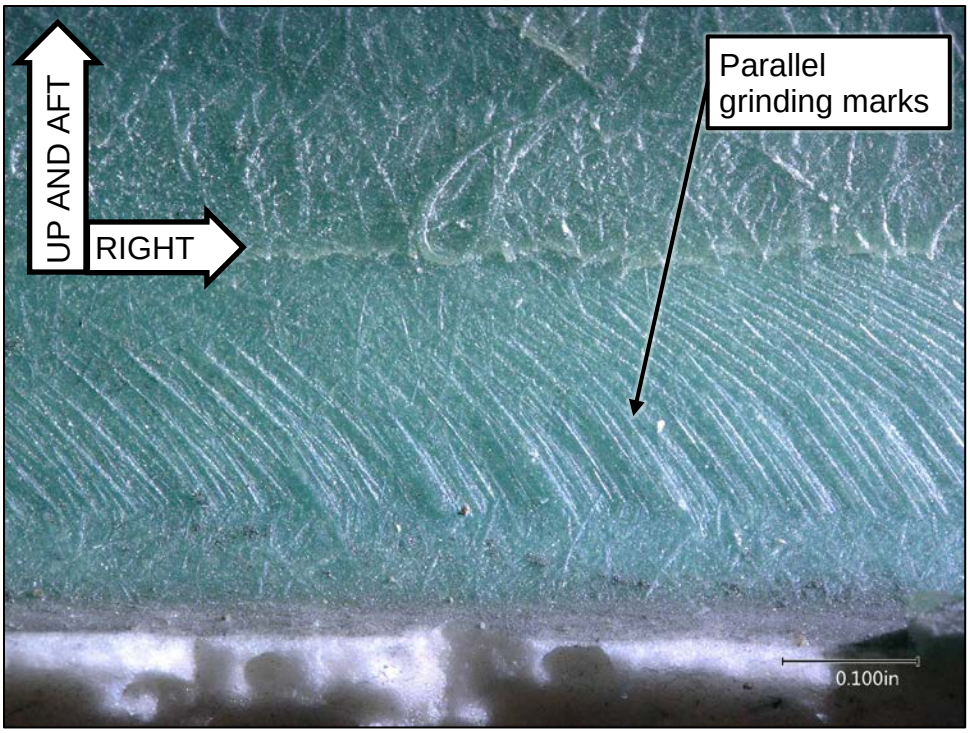

Figure 14. Impressions in the Hysol adhesive corresponding to the edge of the windshield near the forward ends of fractures A and B.

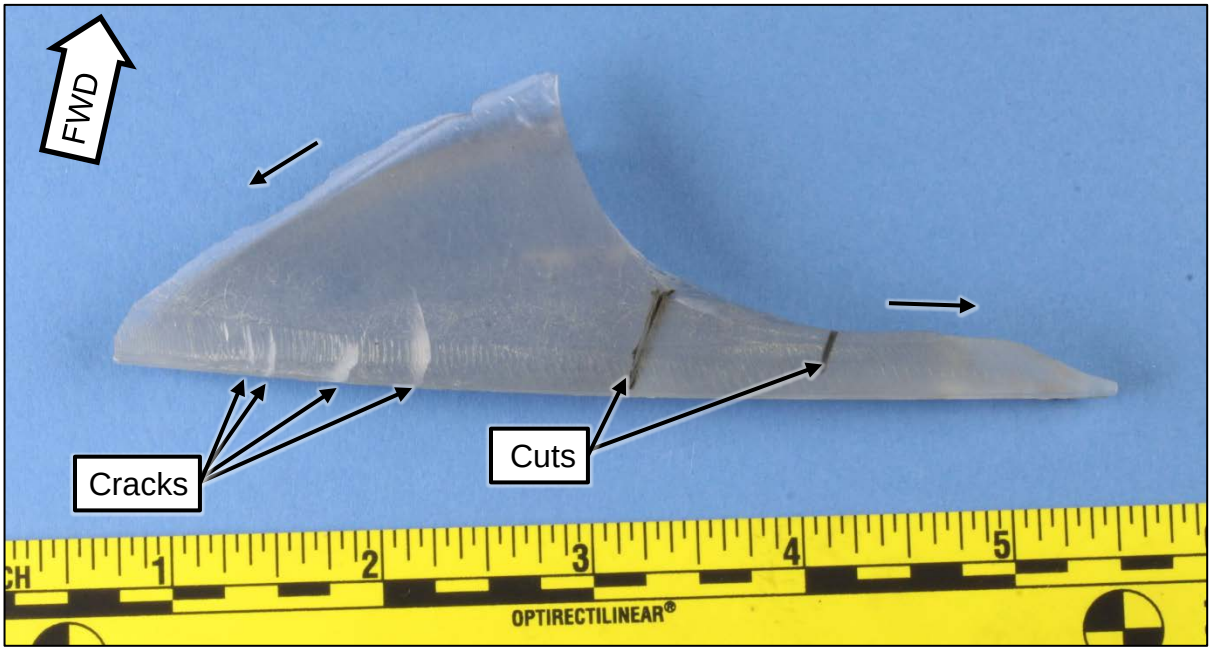

Figure 15. Windshield piece from the upper right side of the windshield at the location indicated in figure 1. Unlabeled arrows indicate directions of fracture propagation.

Figure 16. Closer view of cracks in the beveled edge of the windshield piece from the upper right side of the windshield.

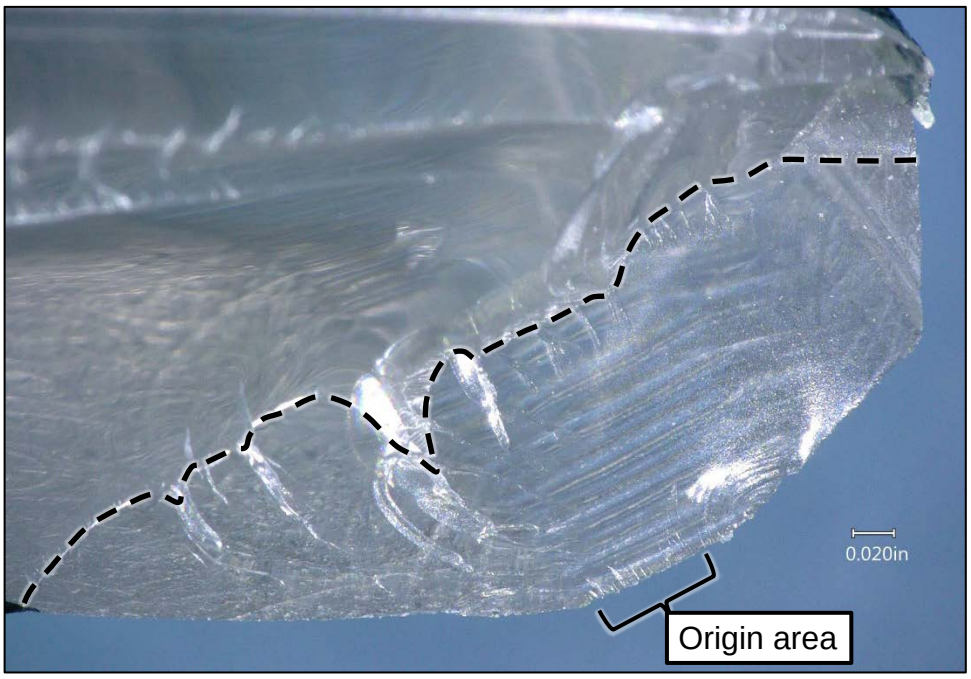

Figure 17. Optical image of the largest crack in the piece from the upper right side after lab fracture. A dashed line indicates the boundary of the crack.

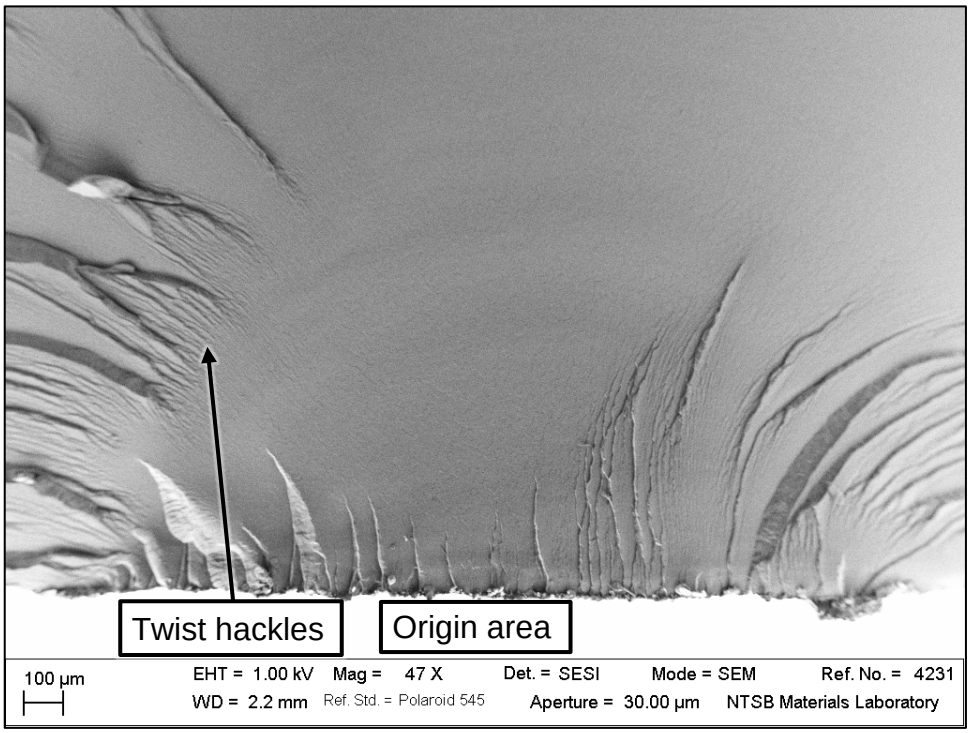

Figure 18. Low-magnification SEM image of the origin area of the lab-opened crack in the windshield piece from the upper right side.

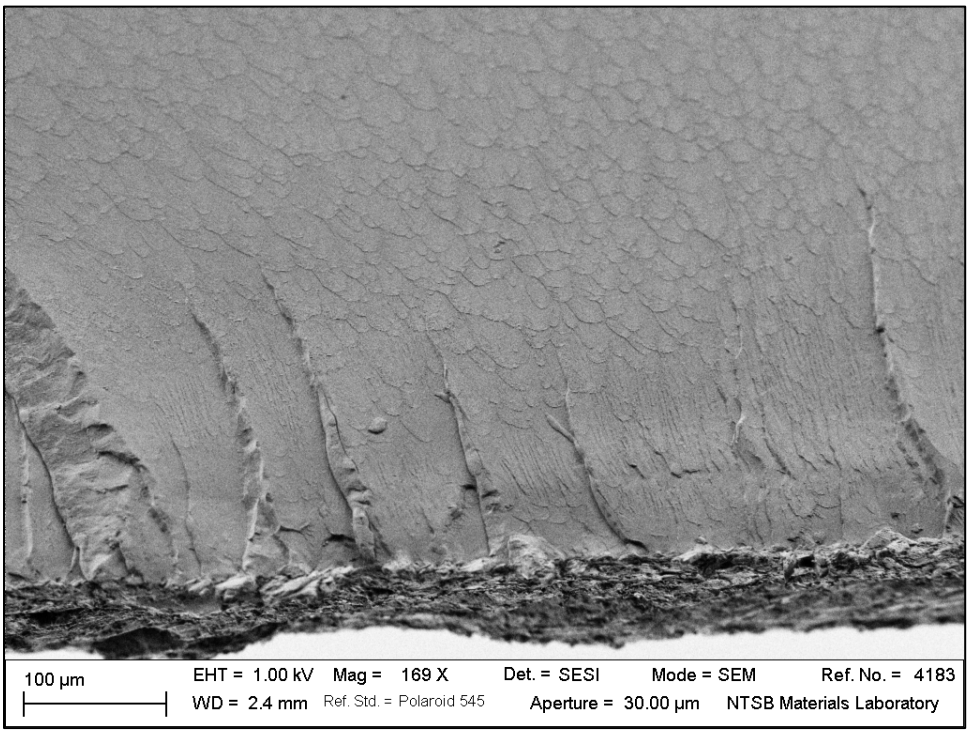

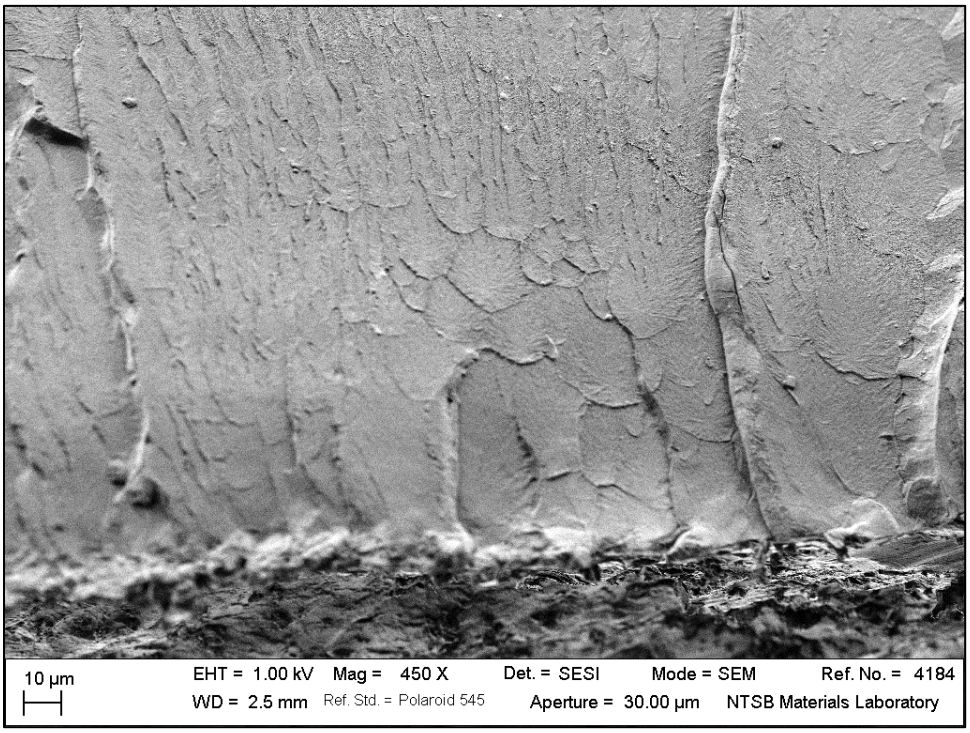

Figure 19. SEM images of the origin area of the lab-opened crack in the windshield piece from the upper right side shown at higher magnification.

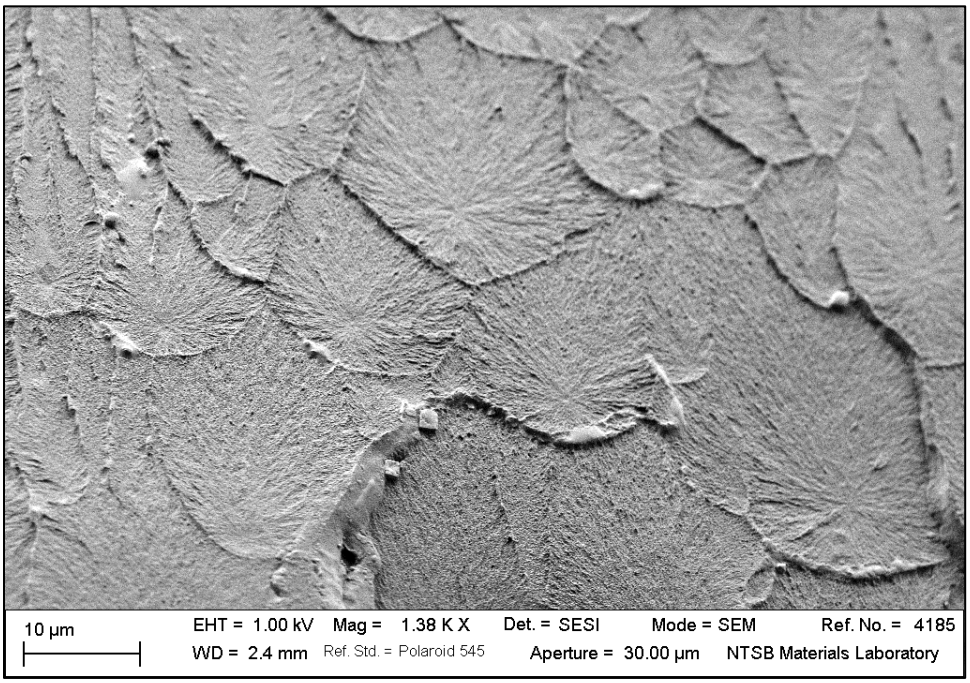

Figure 20. Higher-magnification SEM image of parabolic marks near the origin area of the lab-opened crack in the windshield piece from the upper right side.

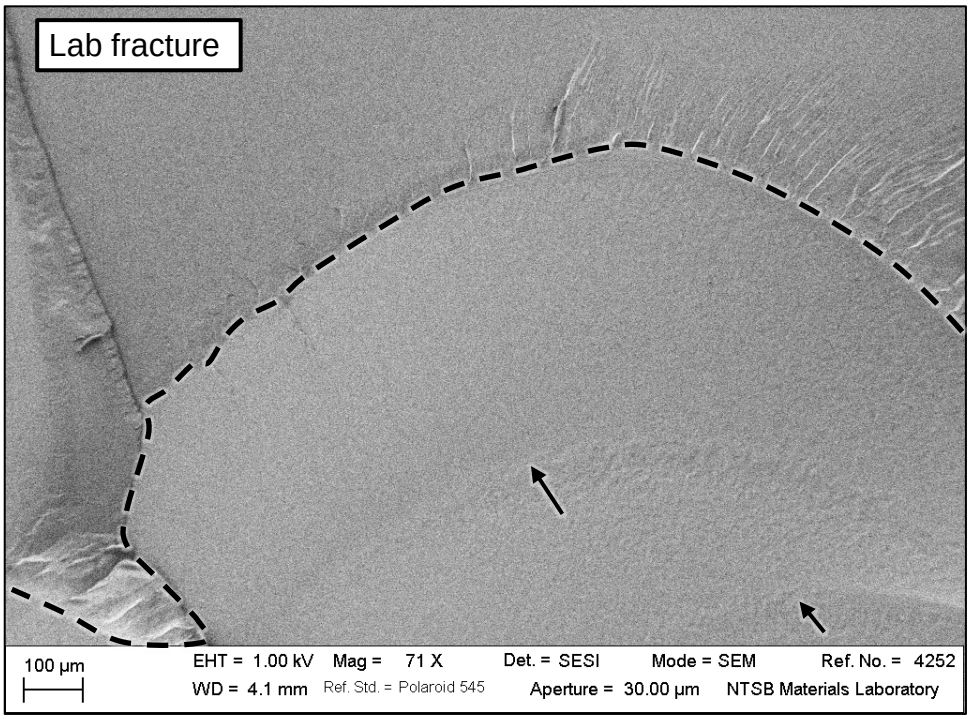

Figure 21. SEM image of the crack boundary of the lab-opened crack in the windshield piece from the upper right side. A dashed line indicates the crack boundary, and unlabeled arrows indicate rib marks on the crack fracture surface.

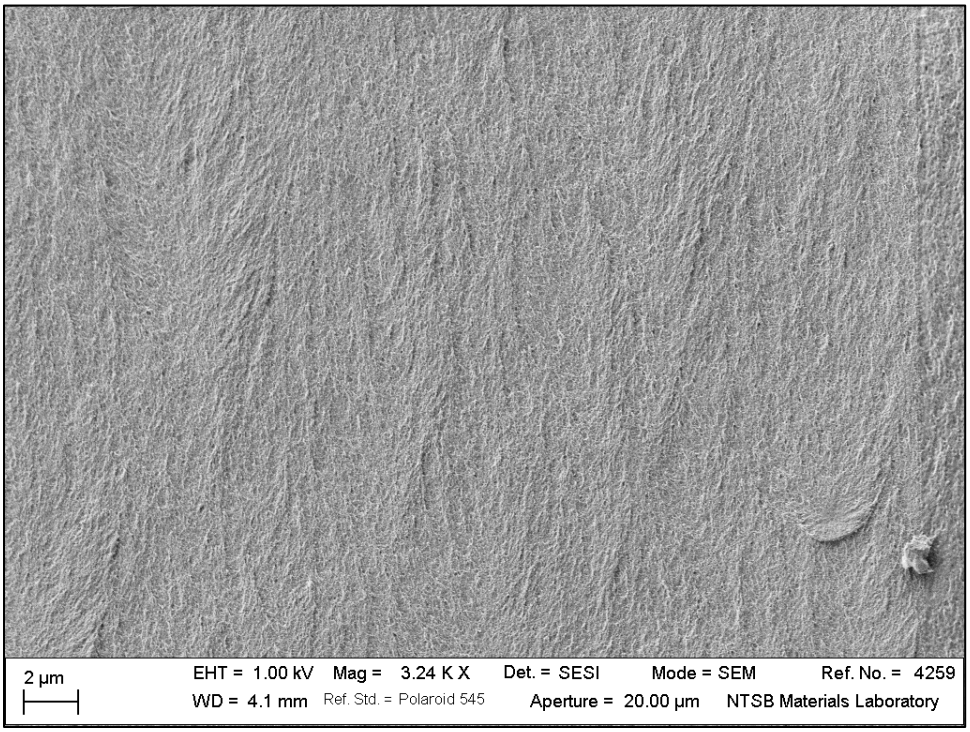

Figure 22. Higher-magnification SEM image of crack fracture features near the crack boundary.

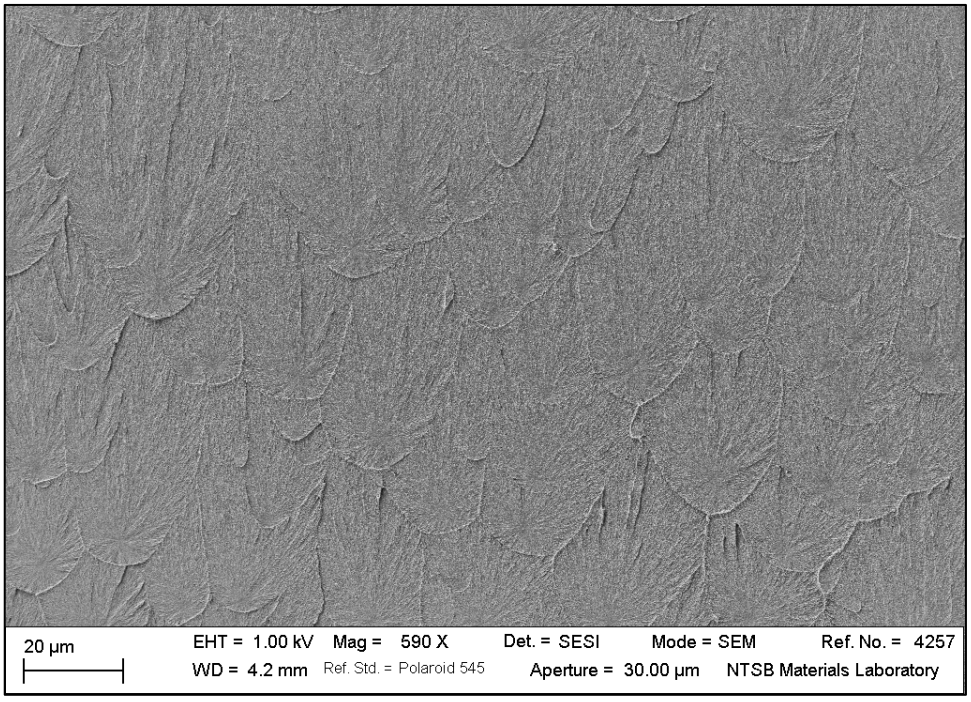

Figure 23. SEM image of fracture features in the lab-fractured portion of the opened crack in the piece from the upper right side of the windshield.

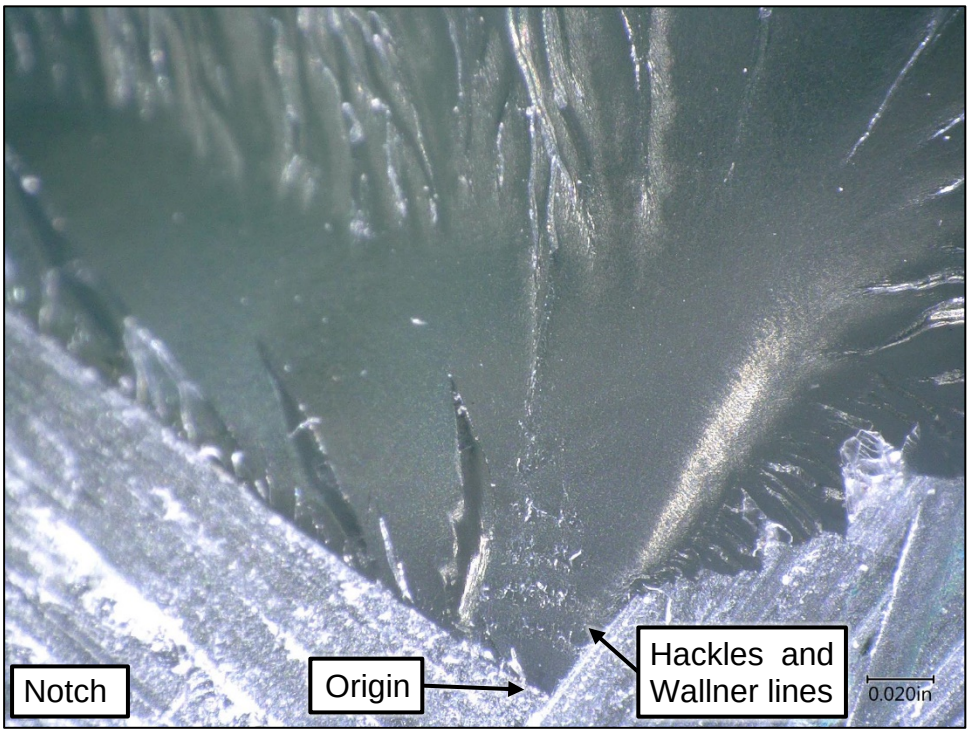

Figure 24. Optical image of a lab-created impact fracture that initiated from a chevron-shaped notch cut into a sample of the windshield.

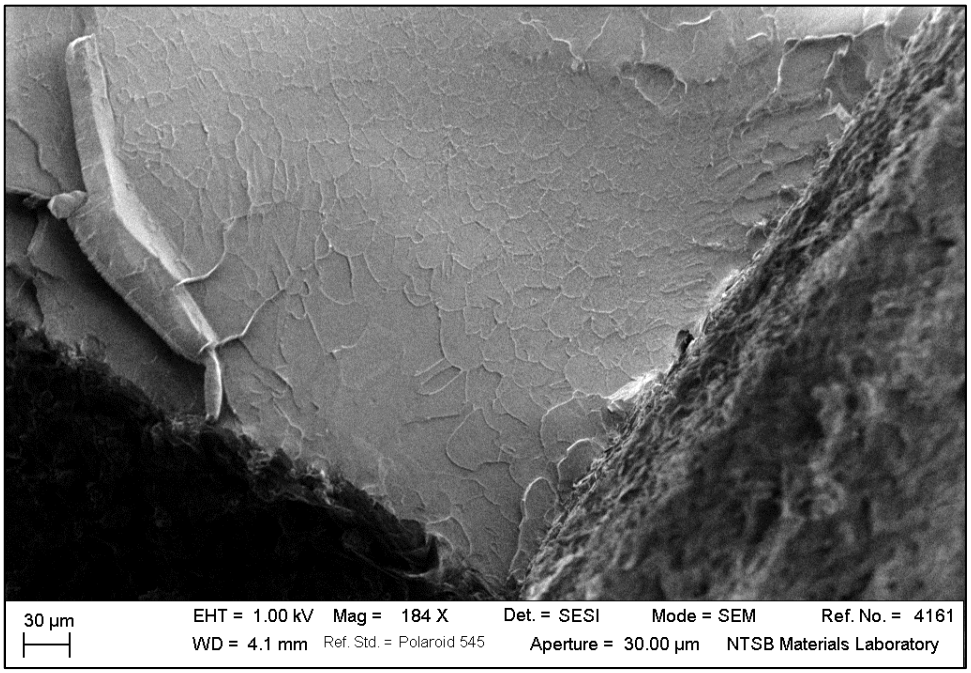

Figure 25. SEM image of the origin of the lab-fractured impact specimen.

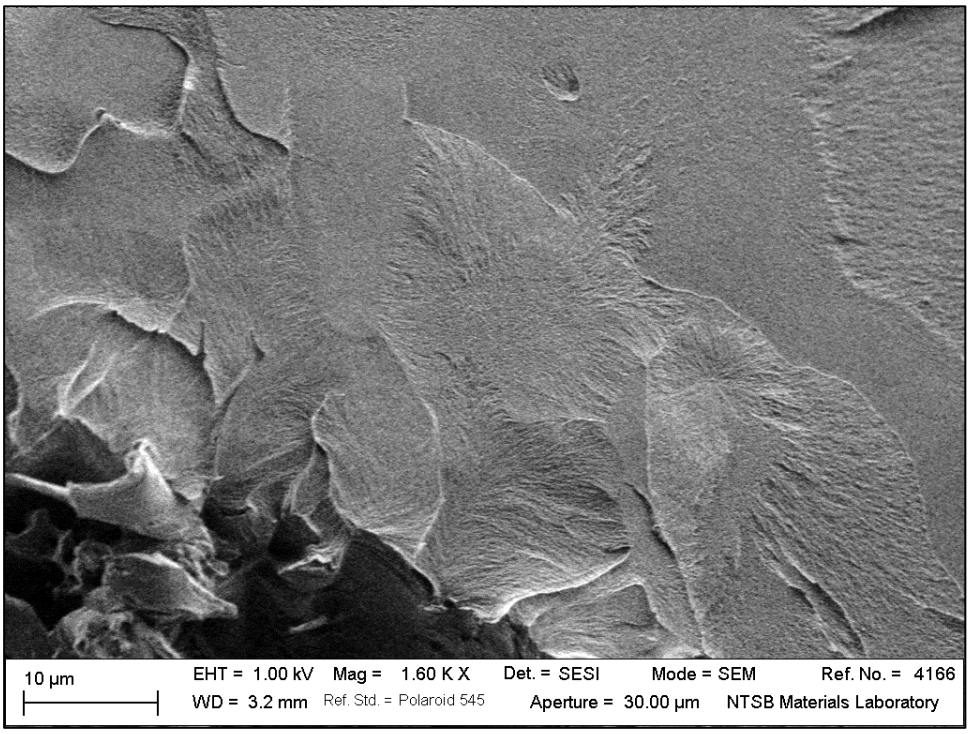

Figure 26. Higher magnification SEM image of the origin area of the lab-fractured impact specimen.

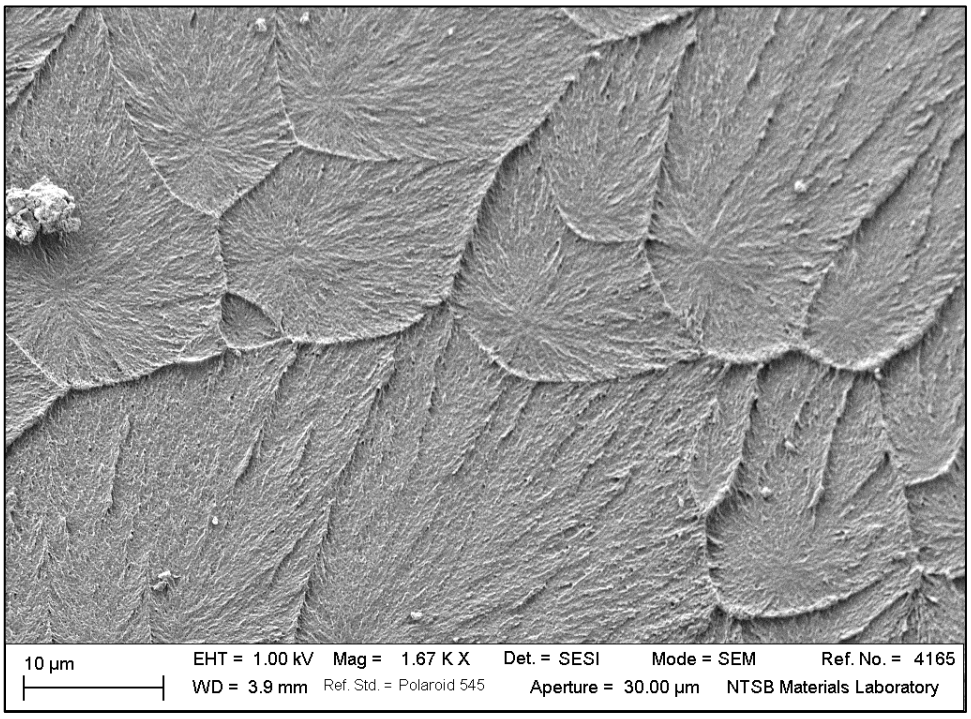

Figure 27. Higher-magnification SEM image of parabolic marks near the origin area of the lab-fractured impact specimen.

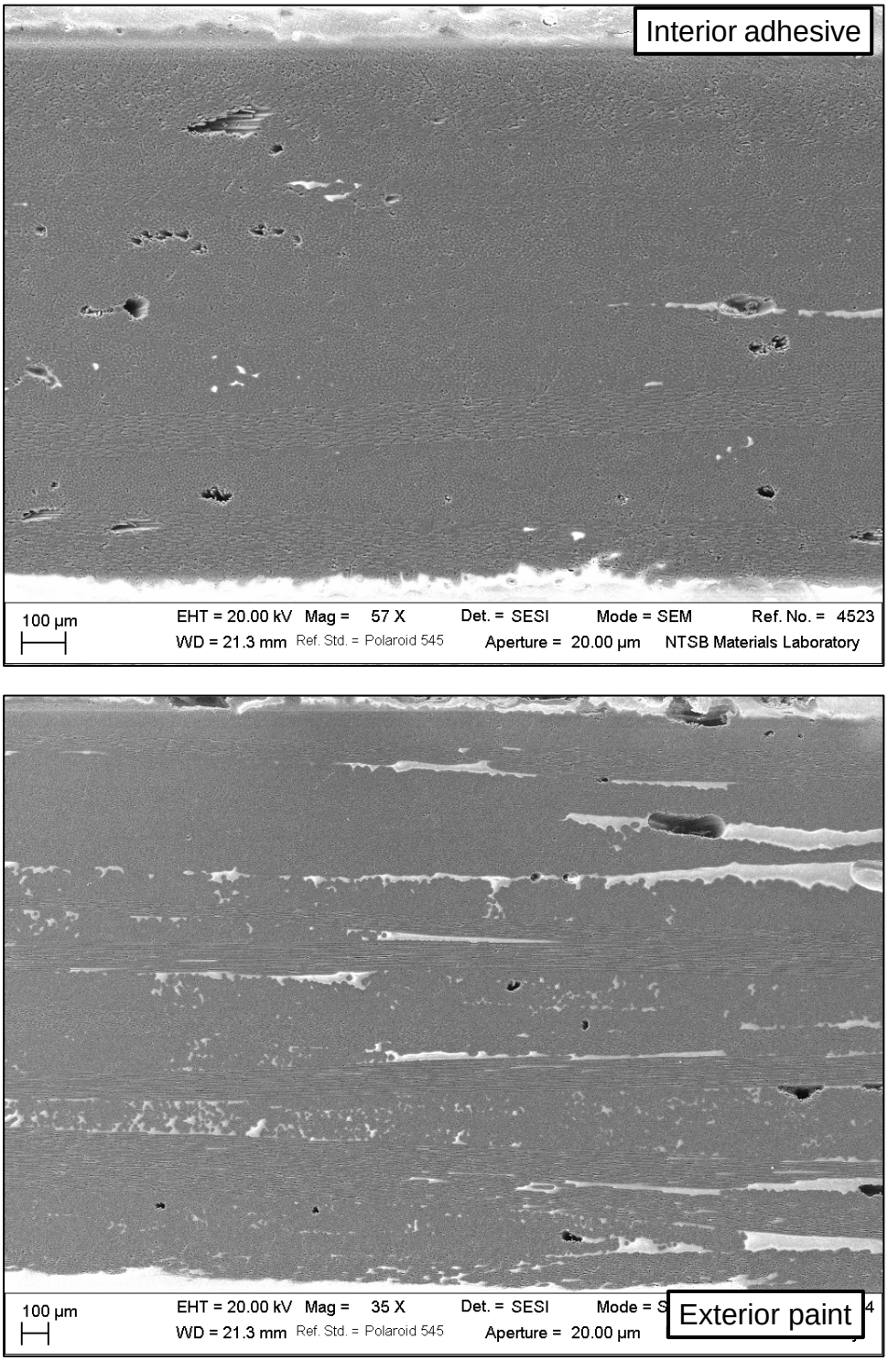

Figure 28. SEM images of a cross-section of the fuselage skin layers showing the interior skin layers (upper image) and the exterior skin layers (lower image).